GDCh Communications Angewandte International Edition Chemie

VIP Gold Nanoclusters Very Important Paper

International Edition: DOI: 10.1002/anie.201805695
German Edition: DOI: 10.1002/ange.201805695

Enantioseparation of $Au_{20}(PP_3)_4Cl_4$ Clusters with Intrinsically Chiral Cores

Yanfei Zhu, Hui Wang, Kaiwei Wan, Jun Guo,Chunting He, Yue Yu, Luyang Zhao, Yin Zhang, Jiawei Lv, Lin Shi, Renxi Jin, Xinxiang Zhang, Xinghua Shi, and Zhiyong Tang*

- CAS Key Laboratory of Nanosystem and Hierarchical Fabrication,
- CAS Center for Excellence in Nanoscience National Center for Nanoscience and Technology Beijing;
- University of Chinese Academy of Sciences Beijing;
- College of Chemistry and Molecular Engineering Peking University, Beijing;
- School of Chemistry, Sun Yat-Sen University Guangzhou

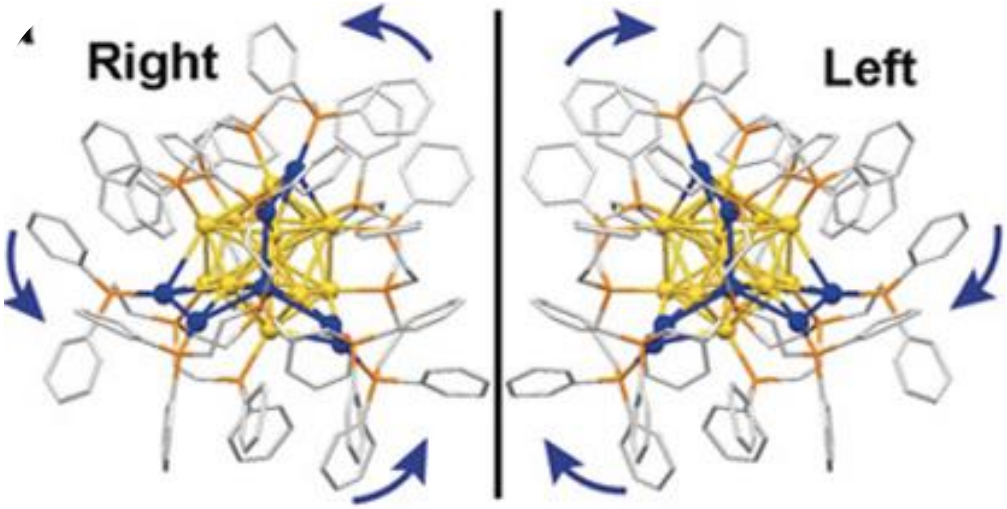

First published: 06 June 2018

Angew. Chem. Int. Ed. **2018**, 57, 9059 –9063

Esma Khatun
13/10/18

Introduction

- Chirality is ubiquitous in nature and pervades much of modern science. Unlike the extensively studied molecular chirality and that of the microscopic helix, the nanoscale chirality between them remains largely uninvestigated.

- Although significant advances have been achieved in this field, the chiral evolution from molecules to nanostructures, as well as the corresponding influence on their properties are not clearly elucidated yet.

- It is suggested that atomically precise chiral Au nanoclusters would become an ideal platform at the nanoscale for understanding the chiral transfer across the organic–inorganic interface and structure–property relationships.

- Chirality could arise because of the following four reasons: (i) ligands arrangement on the cluster surface, (ii) cis/trans isomerism in the bridged Au−S rings, (iii) inherent chirality of the cluster core, and (iv) chiral thiolate ligands.

Background

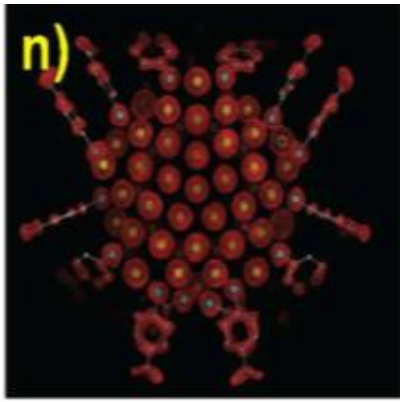

$Au_{102}(p\text{-}MBA)_{44}$

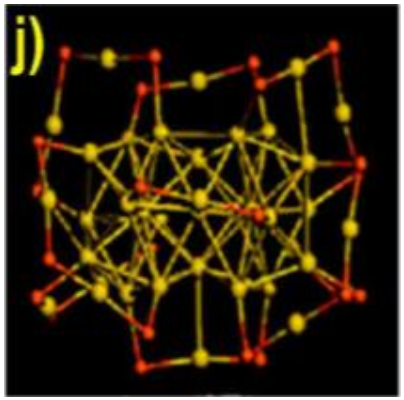

$Au_{38}(PET)_{24}$

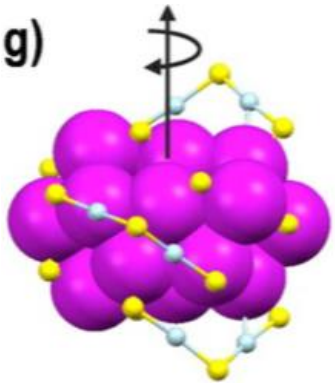

$Au_{28}(TBBT)_{20}$

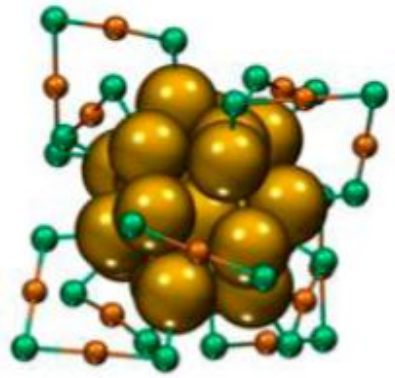

$Au_{40}(2\text{-}PET)_{24}$

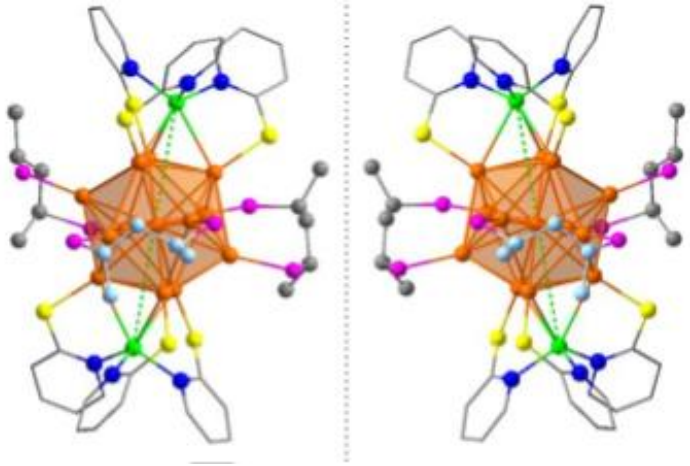

Angewandte Chemie International Edition

10.1002/anie.201800327

WILEY-VCH

COMMUNICATION

From Symmetry Breaking to Unraveling Chirality of Metal Nanoclusters

Guocheng Deng,[a] Sami Malola,[b] Juanzhu Yan,[a] Yingzi Han,[a] Peng Yuan,[a] Chaowei Zhao,[a] Xiting Yuan,[a] Shuichao Lin,[a] Zichao Tang,[a] Boon K. Teo*,[a] Hannu Häkkinen,[b] Nanfeng Zheng*[a]

$[Au_{13}Cu_2(DPPP)_3(SPy)_6]^+$
(2r,4r)/(2s,4s)-DPPP

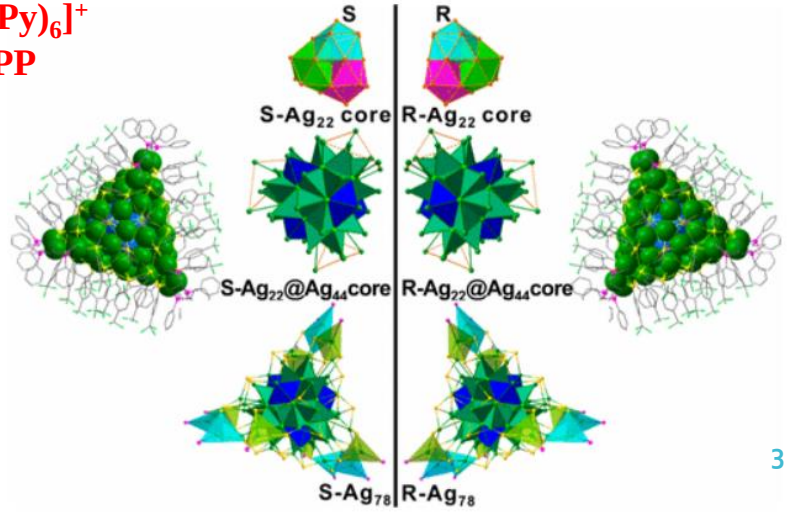

JACS
JOURNAL OF THE AMERICAN CHEMICAL SOCIETY

Communication

Cite This: J. Am. Chem. Soc. 2017, 139, 16113-16116

pubs.acs.org/JACS

From Racemic Metal Nanoparticles to Optically Pure Enantiomers in One Pot

Huayan Yang,† Juanzhu Yan,† Yu Wang, Guocheng Deng, Haifeng Su, Xiaojing Zhao, Chaofa Xu, Boon K. Teo,* and Nanfeng Zheng*

Table S9. Anisotropy factor of the reported chiral Au clusters.

Cluster	Wavelength	g-factors	Prepare method	References
$Au_{38}(SCH_2CH_2Ph)_{24}$	747 nm	4 x 10^{-3}	Chiral HPLC	6
$Au_{40}(SCH_2CH_2Ph)_{24}$	534 nm	3 x 10^{-3}	Chiral HPLC	7
Au_{102}(p-MBA)$_{44}$	Cannot be calculated [a]		Chiral Phase Transfer	8
Au_{28}(TBBT)$_{20}$	Cannot be calculated [a]		Chiral HPLC	9
Au_{20}(TBBT)$_{16}$	Cannot be calculated [a]		No separation	10
$Au_{30}S$(S-t-Bu)$_{18}$	Cannot be calculated [a]		No separation	11
Au_{40}(O-MBT)$_{24}$	Cannot be calculated [a]		No separation	12
Au_{44}(TBBT)$_{28}$	Cannot be calculated [a]		No separation	13
Au_{44}(2,4-DMBT)$_{26}$	Cannot be calculated [a]		No separation	14
Au_{52}(TBBT)$_{32}$	Cannot be calculated [a]		No separation	12
Au_{130}(p-MBT)$_{50}$	Cannot be calculated [a]		No separation	15
Au_{133}(TBBT)$_{52}$	Cannot be calculated [a]		No separation	16
Au_{246}(p-MBT)$_{80}$	Cannot be calculated [a]		No separation	17
Au_{25}(PET*)$_{18}$	Cannot be calculated [b]		Chiral ligand	18
Au_{25}(Capt)$_{18}$	Cannot be calculated [b]		Chiral ligand	18
Au_{25}(SG)$_{18}$	Cannot be calculated [b]		Chiral ligand	18
Au_{38}(Capt)$_{24}$	747 nm	4 x 10^{-3}	Chiral ligand	19
Au_{38}(SG)$_{24}$	620 nm	1.08 x 10^{-3}	Chiral ligand	19
$[Au_{11}(BINAP)_4Cl_2]^+$	430 nm	1.2 x 10^{-3}	Chiral ligand	20
Au_{10}(R/S-BINAP)$_4$(μ3-S)$_4$]Cl_2	340 nm	1 x 10^{-3}	Chiral ligand	21
$[Au_{24}$[(S/ R)-chiraphos]$_6Cl_4]^{2+}$	500 nm	3 × 10^{-3}	Chiral ligand	22
$Au_{20}(PP_3)_4Cl_4$	325 nm	3.5 x 10^{-3}	Supramolecular assembly	This work

In this paper…

- $Au_{20}(PP_3)_4Cl_4$ (PP_3=tris(2-(diphenylphosphino)ethyl) phosphine), abbreviated as Au_{20}, is the only Au nanocluster with an intrinsically chiral core without achiral environment (chiral ligands or Au-thiolate staples), making it a unique object to understand chiral evolution and explore chiral applications.

- Herein, they report a supramolecular assembly strategy with a cyclodextrin (α-CD) to afford enantiopure Au_{20} in bulk, and an enantiomer excess (ee) value of as-separated Au_{20} of 97%.

- As a result of its high purity, the distinctive optical activity of Au_{20}, which originates from electronic transitions confined in chiral cores, is fully explored.

- Theoretical studies reveals that the enantioseparation results from the preferential self-assembly of α -CD with organic ligands on the surface of right handed Au_{20}.

Relevance to our group

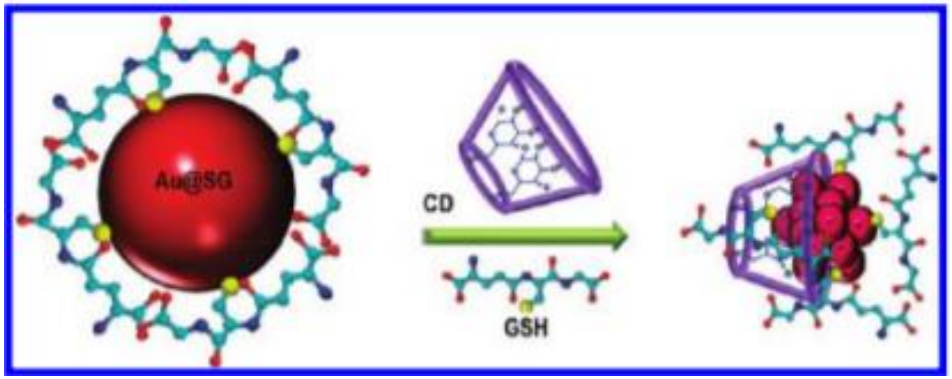

E. S. Shibu, T. Pradeep, Chem. Mater., 23 (2011) 989-999

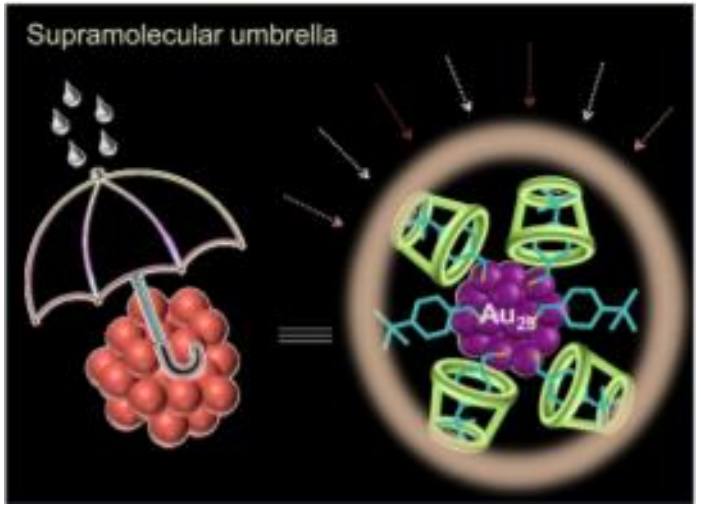

Ammu Mathew *et al*., ACS Nano, 8 (2014) 139-152

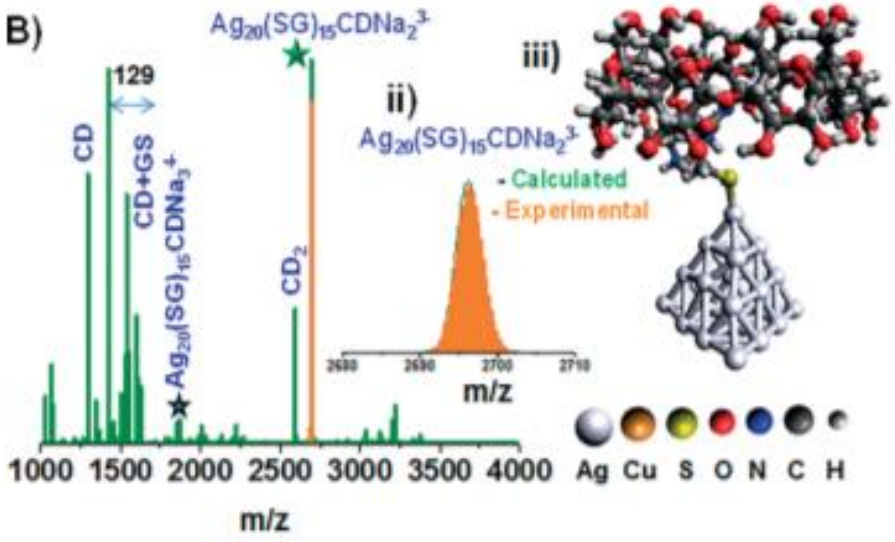

Abhijit Nag *et al*., Eur. J. Inorg. Chem., 2017 (2017) 3072-3079

Synthesis

Inorganic Chemistry
Communication
pubs.acs.org/IC

Synthesis and Structure Determination of a New Au_{20} Nanocluster Protected by Tripodal Tetraphosphine Ligands

Jing Chen, Qian-Fan Zhang, Paul G. Williard, and Lai-Sheng Wang*

Department of Chemistry, Brown University, Providence, Rhode Island 02912, United States

PP_3 =

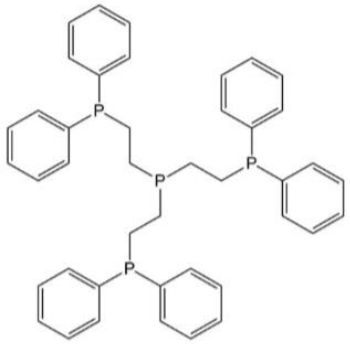

- $Au_4Cl_4PP_3$ complex was firstly synthesized

0.3 mmol PP_3 (45 ml acetone)

1.2 mmol Me_2SAuCl (75 ml acetone)

stirred for about 2 h

A white precipitate

Precipitate was collected by filtration, and washed with acetone, diethyl ether and pentane in sequence

White product was dried under vacuum to get the $Au_4Cl_4PP_3$ complex.

- Synthesis of $Au_{20}(PP_3)_4Cl_4$

32 mg $Au_4Cl_4PP_3$ in 25 mL DCM

heated to 50°C

A clear solution

Addition of $NaBH_4$ (ethanol)

After 4 h

DCM was evaporated and washed several times with DCM-toluene mixture

Structure of $Au_{20}(PP_3)_4Cl_4$

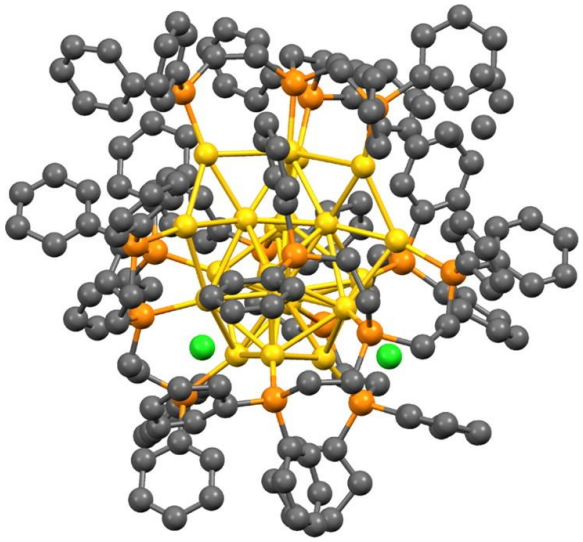

Total structure of $Au_{20}(PP_3)_4Cl_4$.

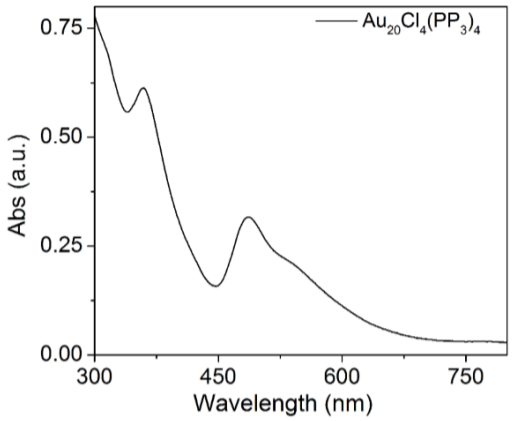

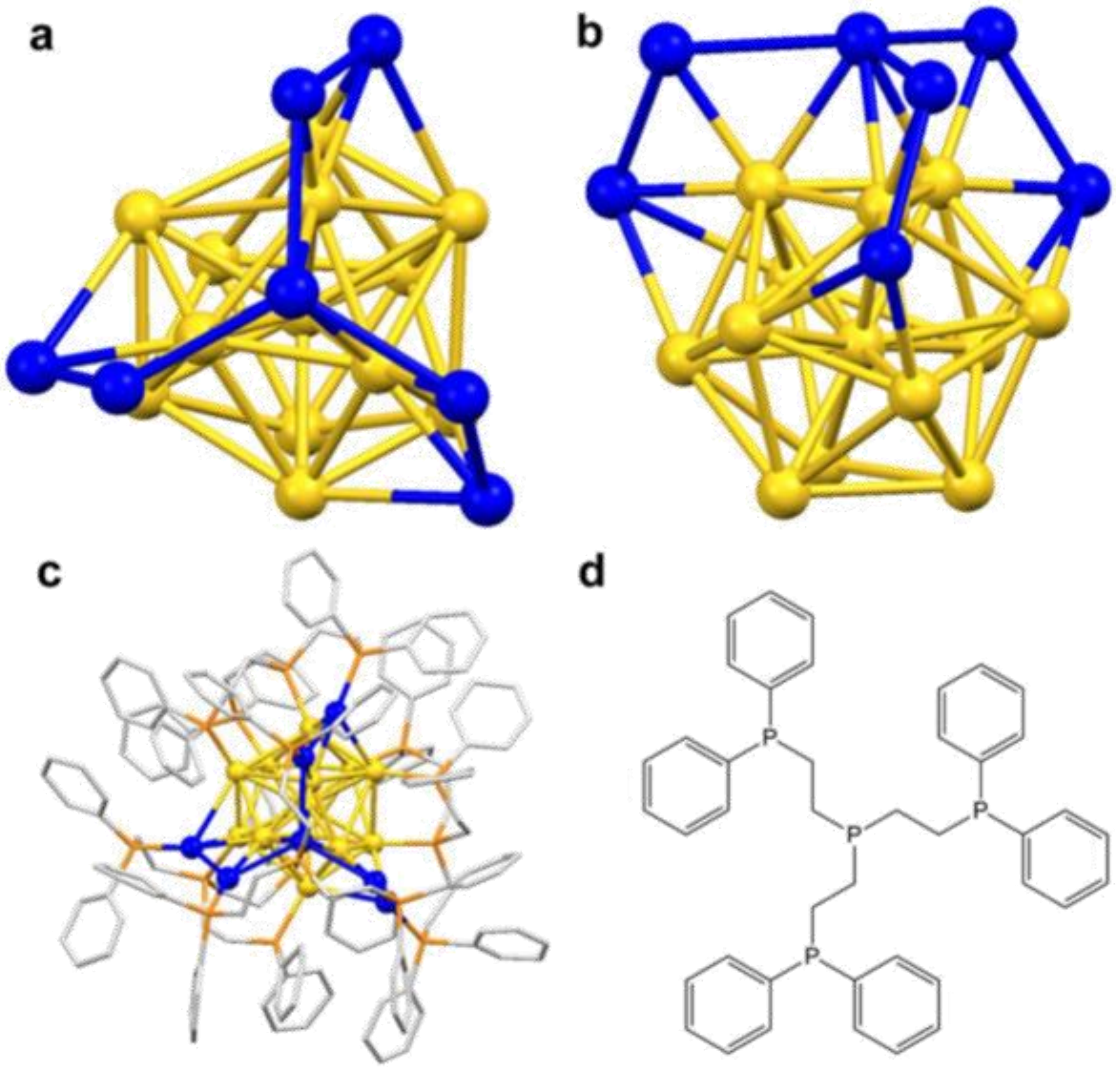

Figure S1. (a) Top view of Au_{20} core, and chirality of Au atoms is highlighted in blue. (b) Side view. (c) Top view of $[Au_{20}(PP_3)_4]^{4+}$. (d) Structure of tris(2-(diphenylphosphino)ethyl)phosphine (PP_3) ligand. Color labels: golden and blue, Au; orange, P; gray, C. H atoms are omitted.

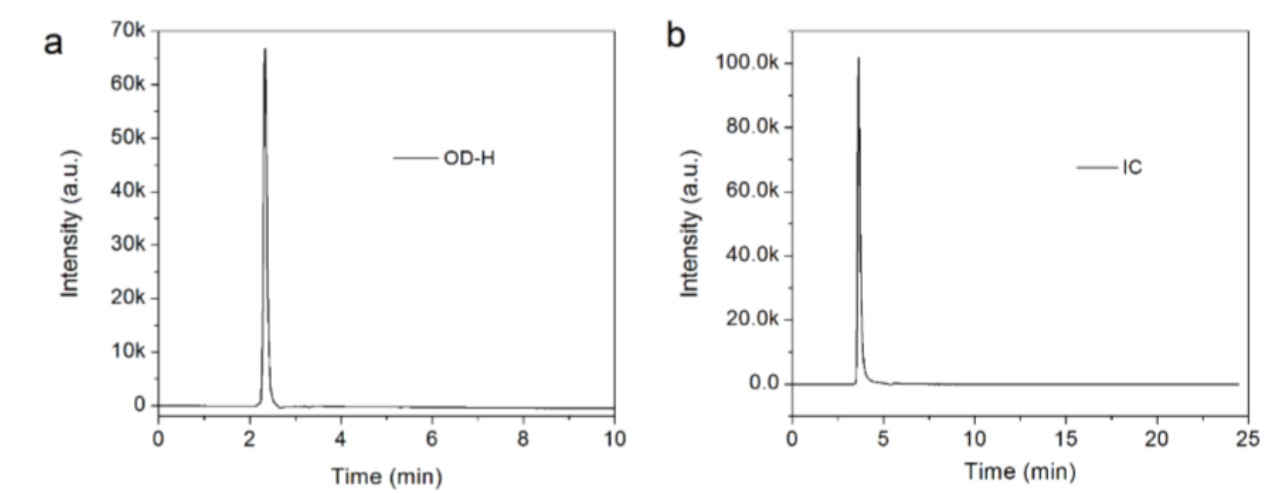

Figure S3. (a) HPLC chromatogram of enantioseparation of racemic Au_{20} with Chiralcel OD-H column (5 μm, 4.6 mm × 250 mm). (b) HPLC chromatogram of enantioseparation of racemic Au_{20} with Chiralcel IC column (5 μm, 4.6 mm × 250 mm).

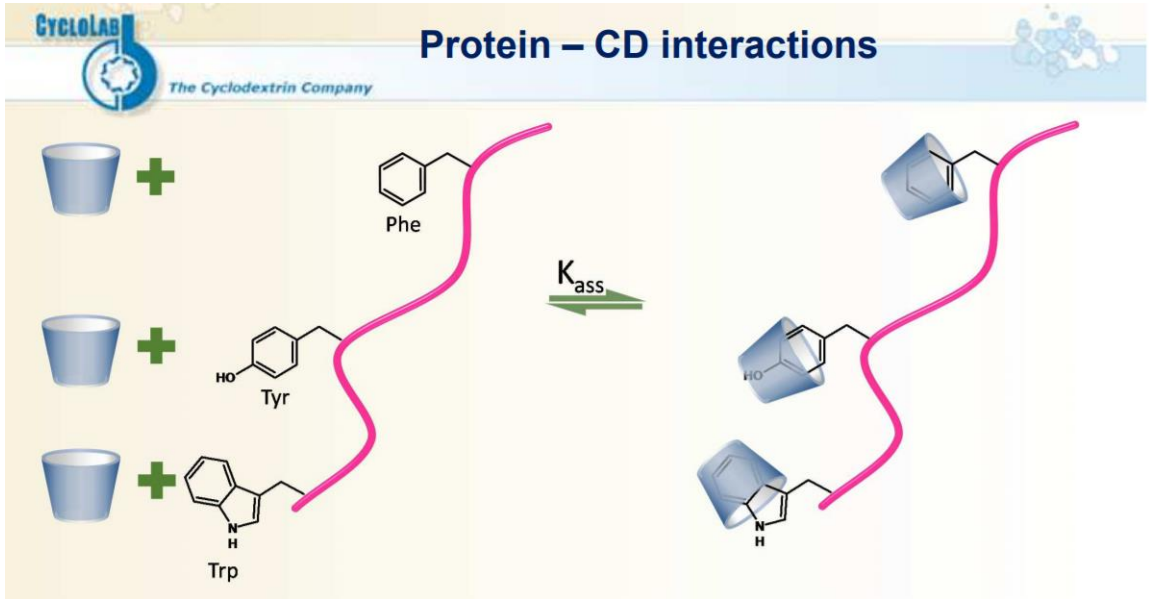

Separation

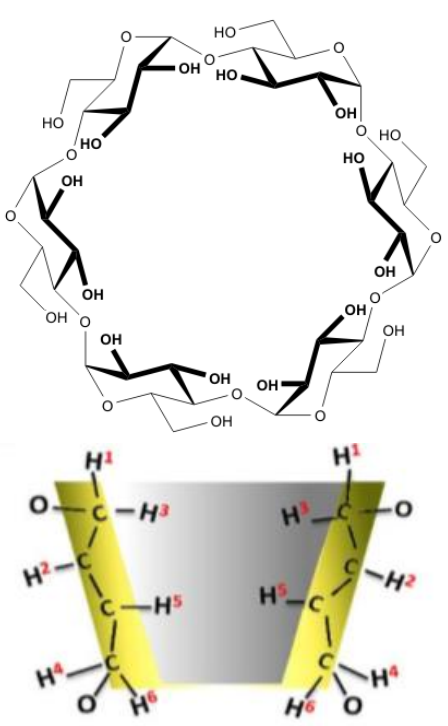

α-Cyclodextrin

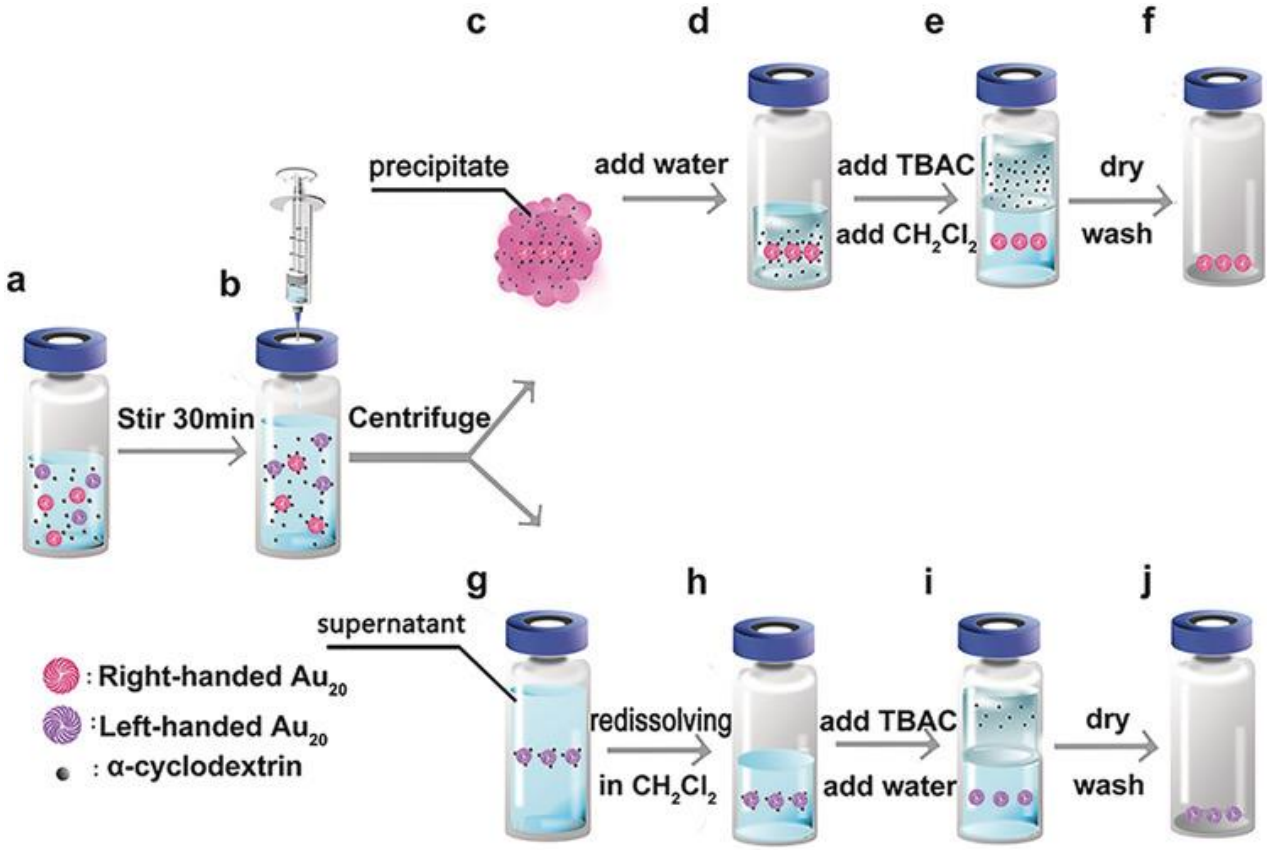

Figure 1. a) Dissolving Au_{20} and α-CD in DMF. b) Stirring and adding CH_2Cl_2 as a poor solvent. c) Centrifuging to isolate the precipitate (enriched R-Au_{20}) d) Dissolving precipitate in water. e) Transferring R-$Au_{20}$from water to CH_2Cl_2 with aid of TBAC (to remove bound α-CD). f) Acquiring bare R-Au_{20}via drying and washing by water to remove TBAC. g) Centrifuging to collect supernatant solution (enriched L-Au_{20}). h) Re-dissolving in CH_2Cl_2. i) Removing residual α-CD in L-$Au_{20}(\alpha\text{-CD})_n$ with TBAC. j) Acquiring bare L-Au_{20} via drying and washing by water to remove TBAC. Solvents: blue CH_2Cl_2 or DMF; gray H_2O.

Characterizations

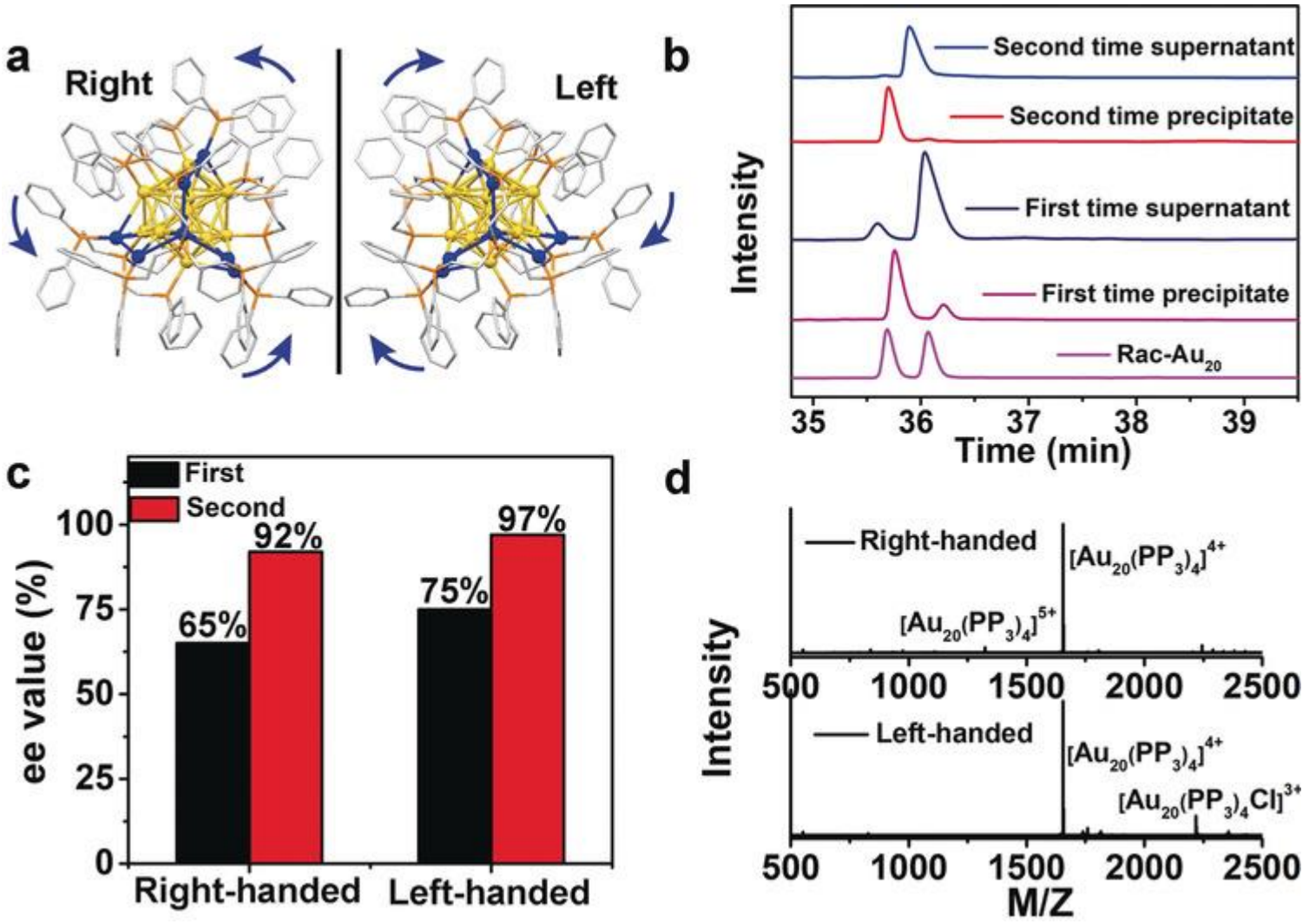

Figure 2. a) Structure of two enantiomers of Au_{20}. b) Electropherograms of racemic Au_{20}, precipitate, and supernatant after the first and second separation (from bottom to top). c) The *ee* value of products after the first and second enantioseparation processes. d) ESI-MS spectra of R-Au_{20} and L-Au_{20}.

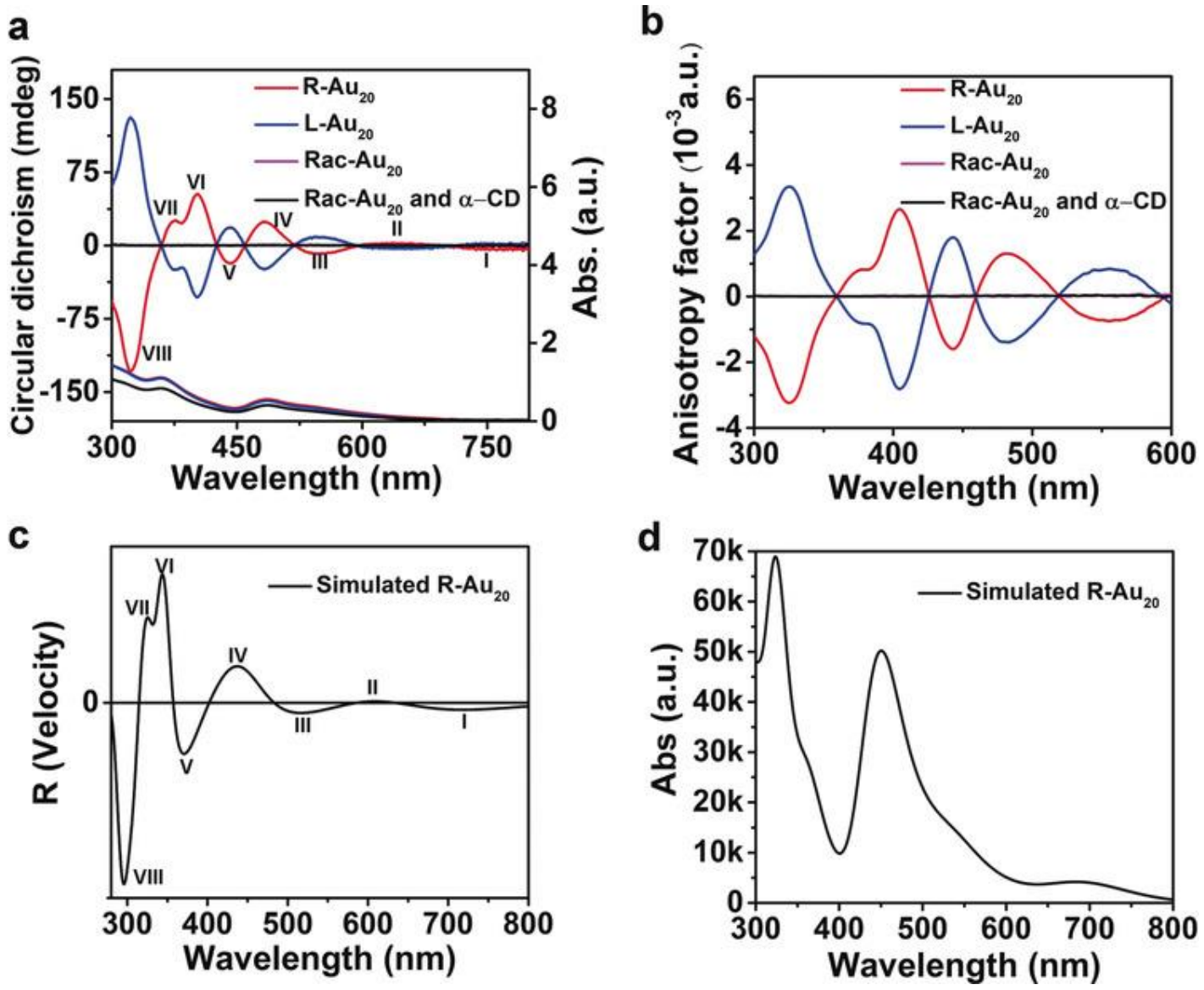

Figure 3. a) Experimental circular dichroism and UV/Vis spectra of racemic Au_{20} (*rac*-Au_{20}), mixture of racemic Au_{20} and α-CD, R-Au_{20}, and L-Au_{20}. b) Experimental g-factors. c) Simulated circular dichroism spectrum. d) Simulated UV/Vis spectrum.

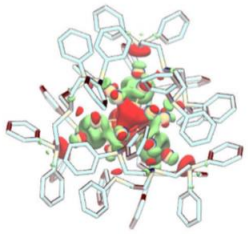

HOMO

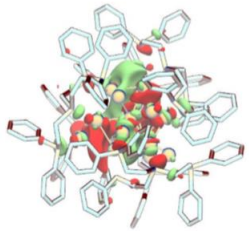

LUMO

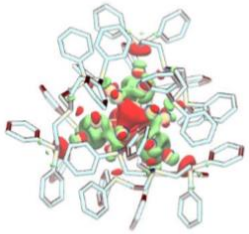

HOMO

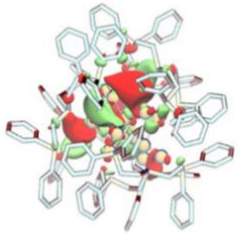

LUMO+4

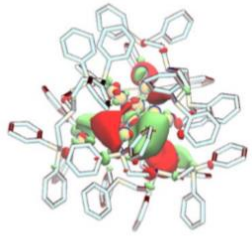

LUMO+5

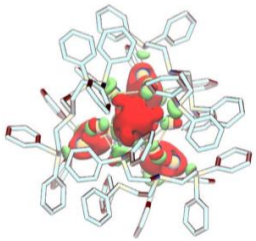

HOMO-1

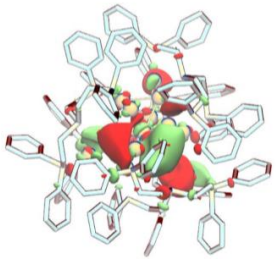

LUMO+5

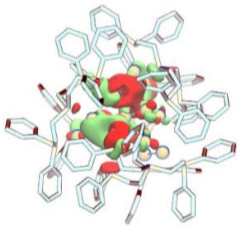

HOMO-3

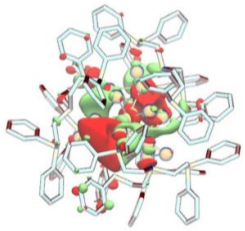

LUMO+7

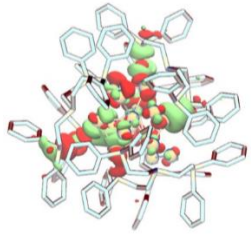

HOMO-9

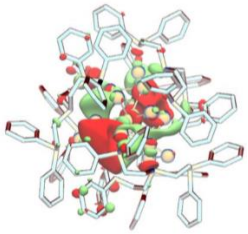

LUMO+7

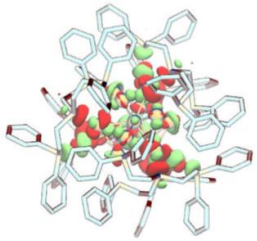

HOMO-4

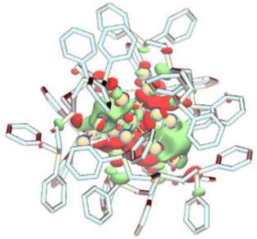

LUMO+1

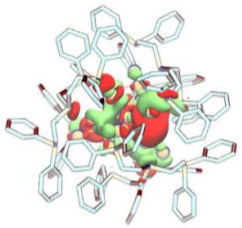

HOMO-2

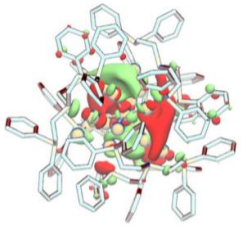

LUMO+6

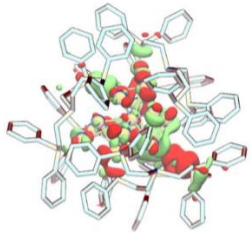

HOMO-8

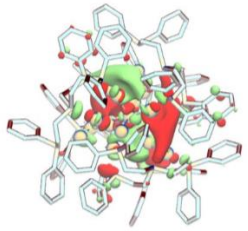

LUMO+6

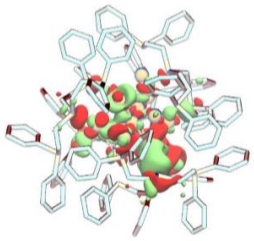

HOMO-5

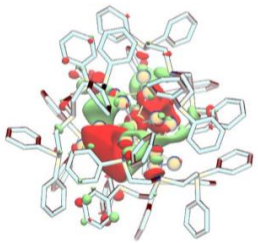

LUMO+7

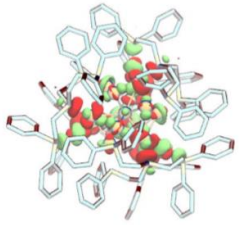

HOMO-4

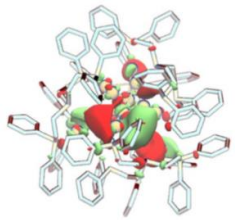

LOMO+5

Figure S14-21

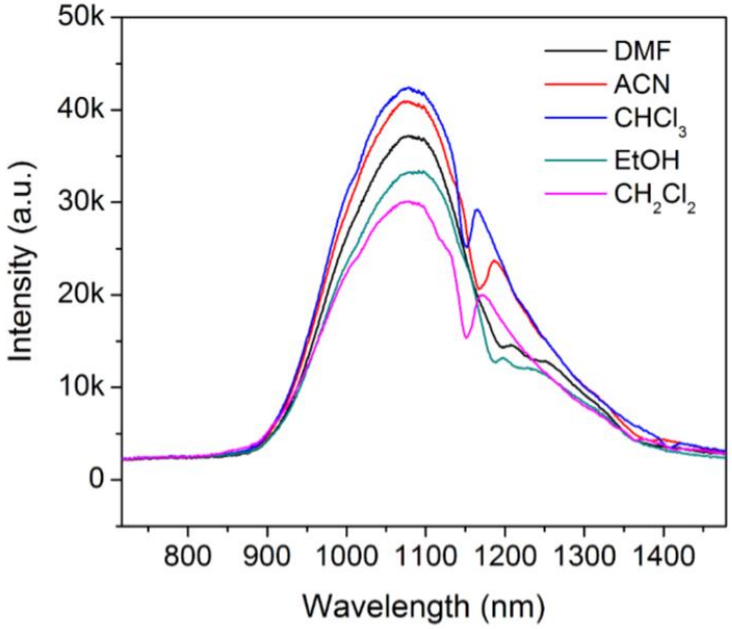

Figure S22. Potoluminescence spectra (λ_{ex} = 480 nm, C_{Au20} = 1.34 × 10-5 M) of Au_{20} in different solvents.

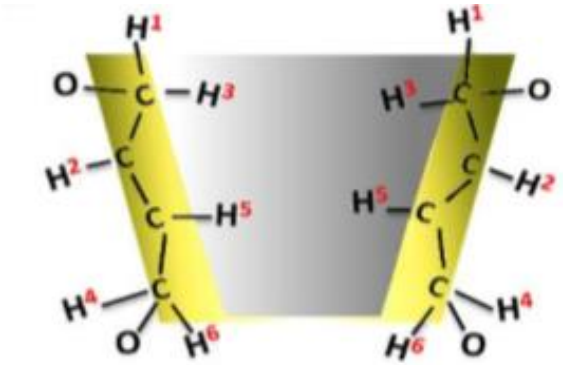

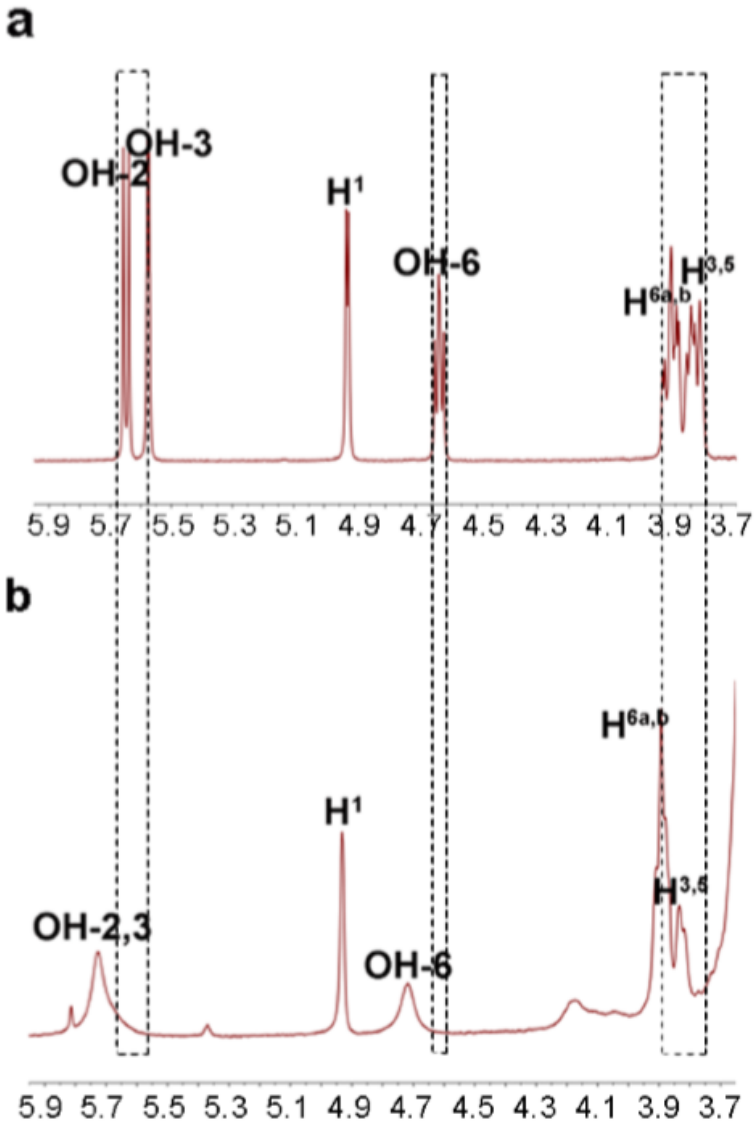

Figure S23. 1H NMR spectra of α-CD in absence and presence of Au_{20} in DMF-d7 at 25 °C, respectively. (a) α-CD. (b) α-CD and Au_{20} (1:1).

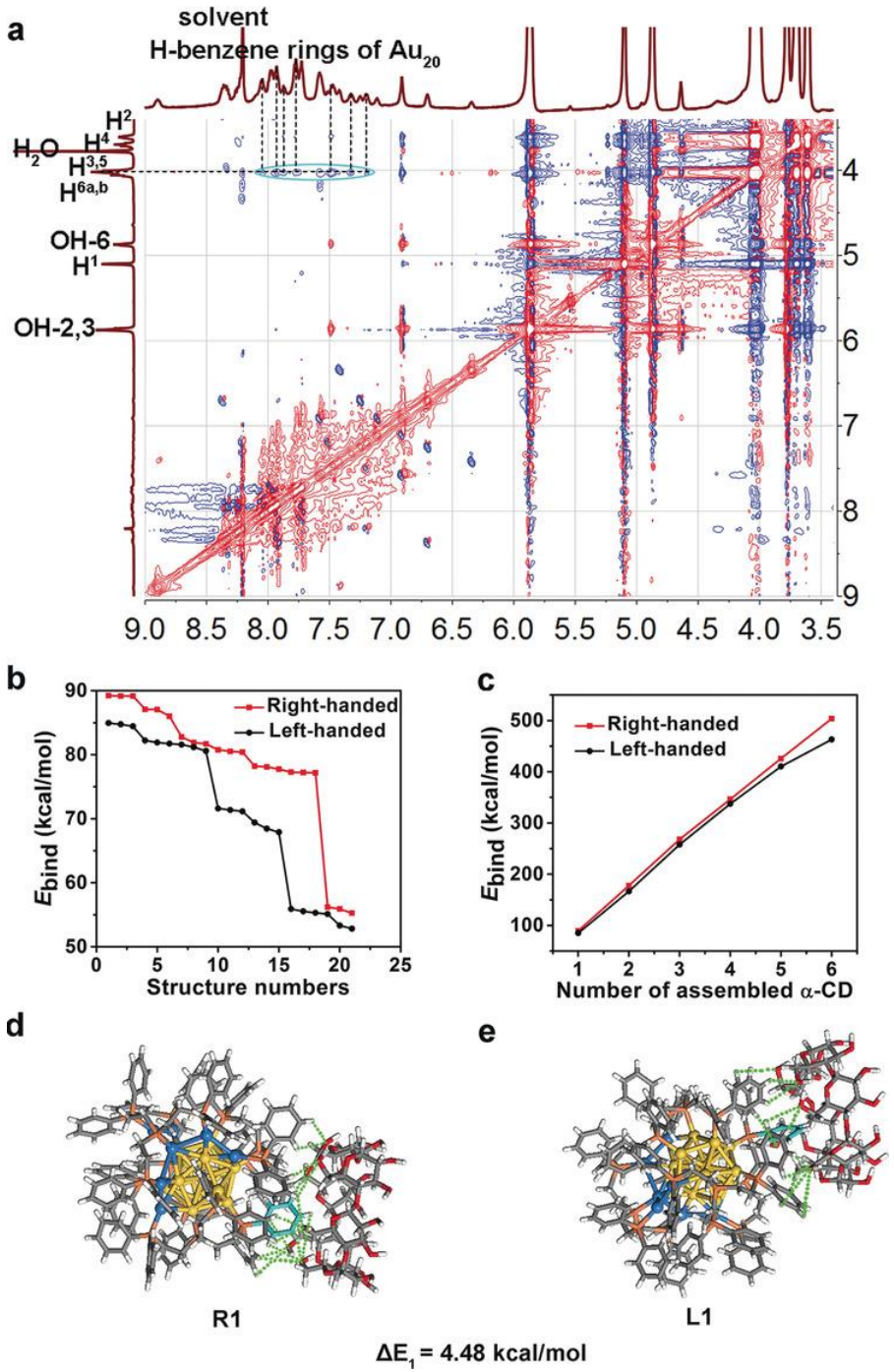

Figure 4. a) Two-dimensional ROESY of α-CD and Au_{20} in [D_7]DMF showing interaction between the inner cavity protons of α-CD and PP_3 ligands (cyan oval). b) Binding energy of R-Au_{20}(α-CD)$_1$ and L-Au_{20}(α-CD)$_1$ at 21 different binding sites. c) Binding energy of R-Au_{20}(α-CD)$_{1–6}$ and L-Au_{20}(α-CD)$_{1–6}$ with preferred configuration. d),e) The most stable configuration of R-Au_{20}(α-CD)$_1$ and L-Au_{20}(α-CD)$_1$ assemblies, abbreviated as, R1 and L1, respectively (the cyan benzene ring is the one which inserts into the cavity of α-CD). Green dashed lines present the interactions between hydroxy groups of α-CD and hydrogen atoms of benzene rings. Au gold or blue, P orange, C gray, O red, H white.

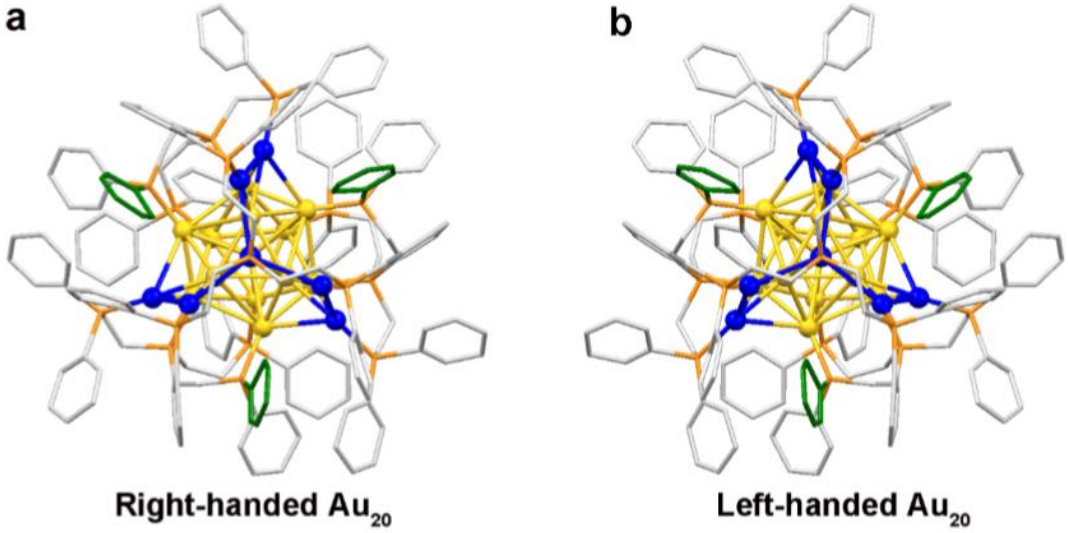

Figure S25. (a) Schematic structures of three benzene rings (green) of R-Au20 that couldn't insert into α-CD according to molecular docking simulation. (b) Schematic structures of three benzene rings (green) of L-Au20 that couldn't insert into α-CD according to molecular docking simulation. Color labels: golden and blue, Au; orange, P; gray, C. H atoms are omitted.

Figure S26. (a), (b) Structures of 7 triangle planes that are composed of three binding sites with similar conformations (green dashed lines). (c), (d) Corresponding structures without ligands. Color labels: golden and blue, Au; orange, P; gray, C and H. R-Au_{20} is chosen as the model to show the conformations of 21 binding sites. The vertex of each triangle is the hydrogen atom located on the para-position of phosphorus atom.

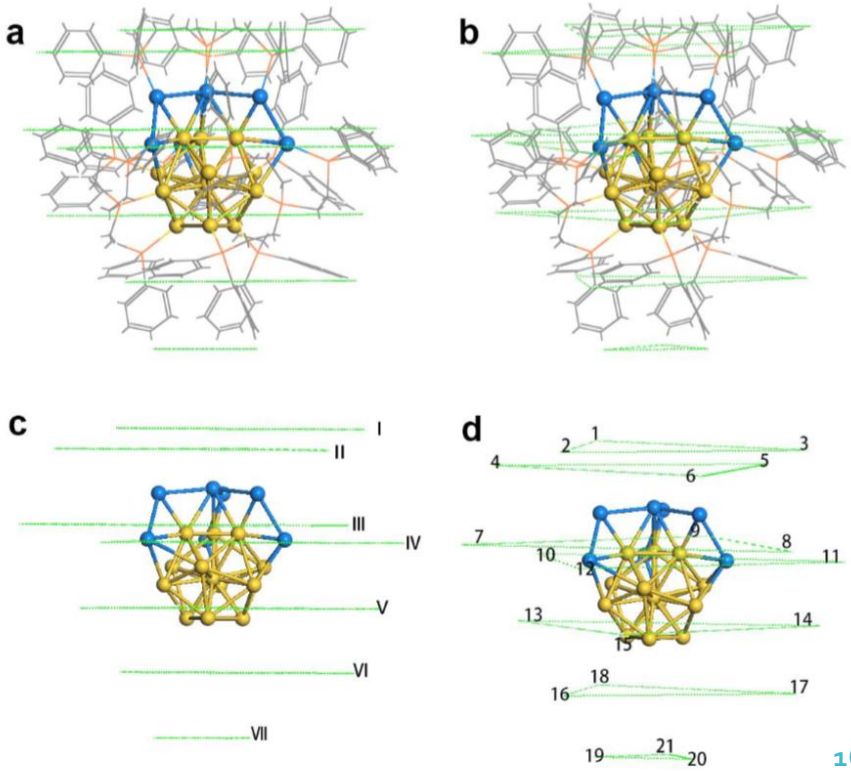

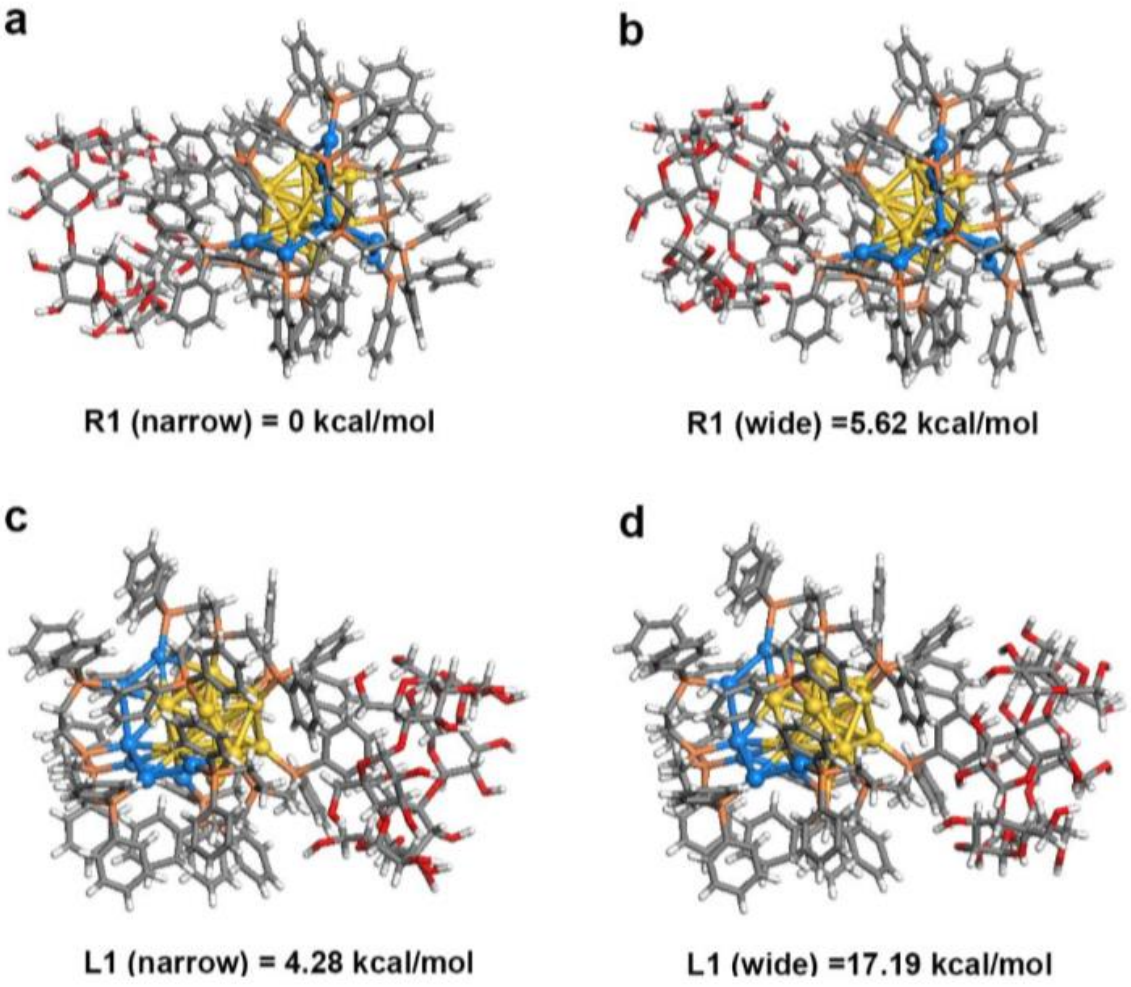

Figure S27. Relative energy and structure of R-Au_{20} or L-Au_{20} assembled with narrow or wide rim of α-CD according to QM calculations. (a) R-Au_{20} assembled with narrow rim of α-CD. (b) R-Au_{20} assembled with wide rim of α-CD. (c) L-Au_{20} assembled with narrow rim of α-CD. (d) L-Au_{20} assembled with wide rim of α-CD. Color labels: golden and blue, Au; orange, P; gray, C; red, O.

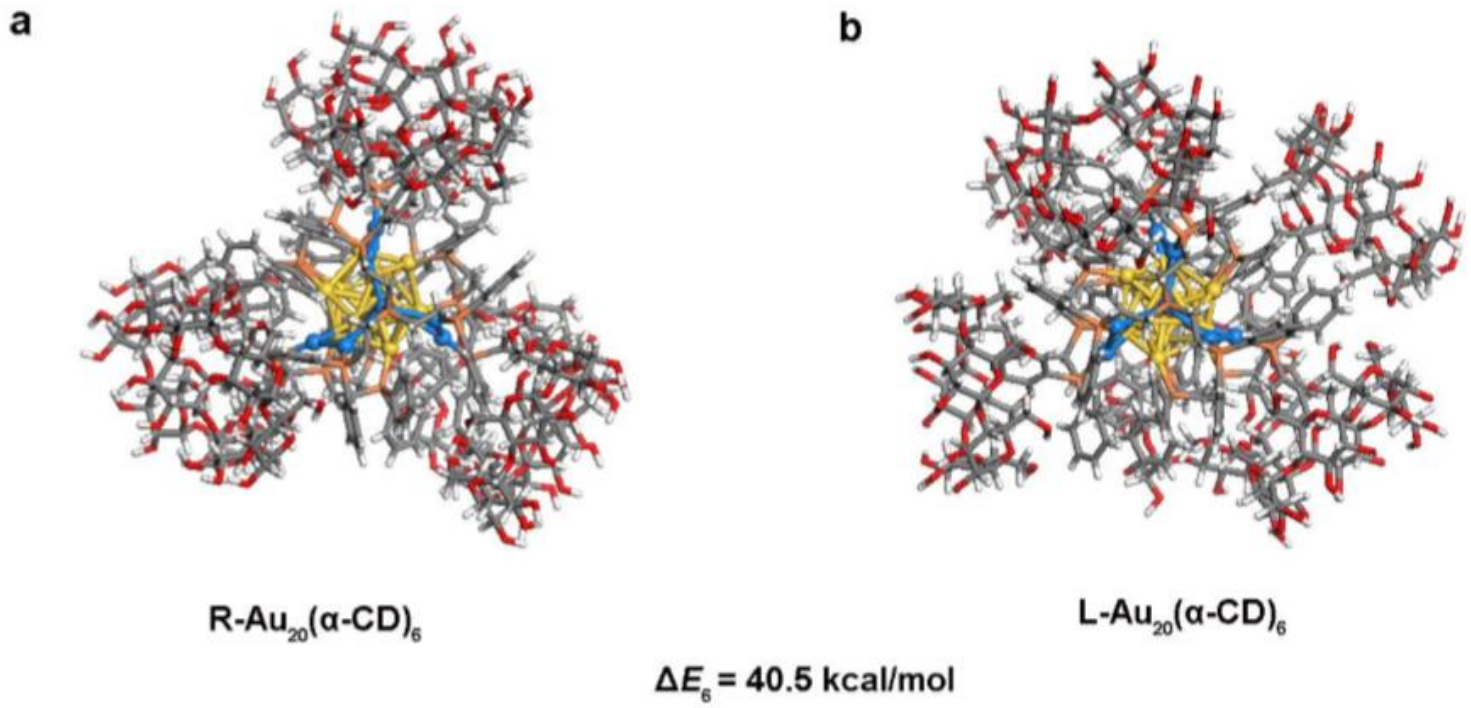

Figure S34. (a) Schematic structures of the most stable R-Au_{20}(α-CD)$_6$ assemblies. (a) Schematic structures of the most stable L-Au_{20}(α-CD)$_6$ assemblies

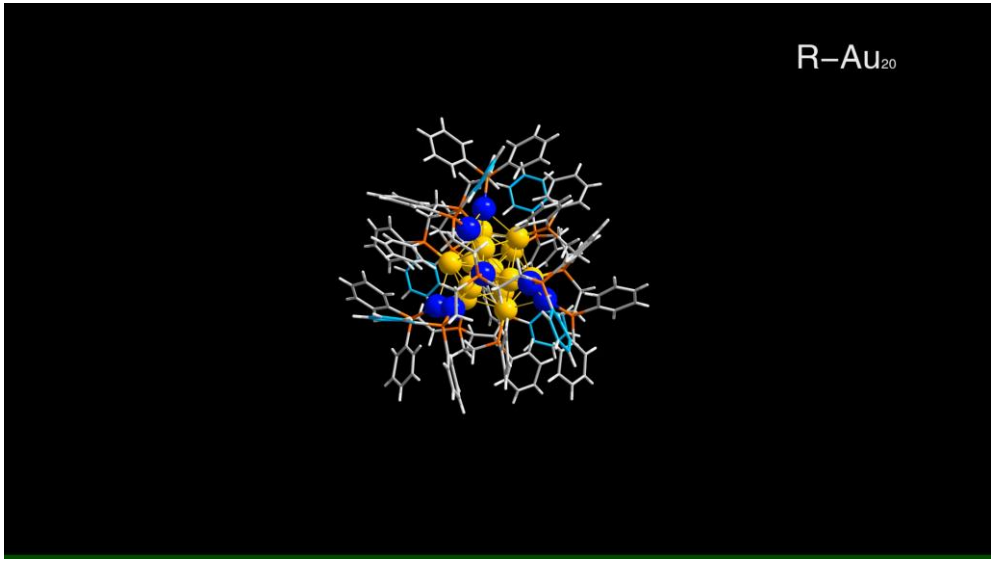

Movie S1. (mp4 format) Movie of molecular docking and quantum-chemistry simulations of the R-Au_{20}(α-CD)$_6$ assembly process.

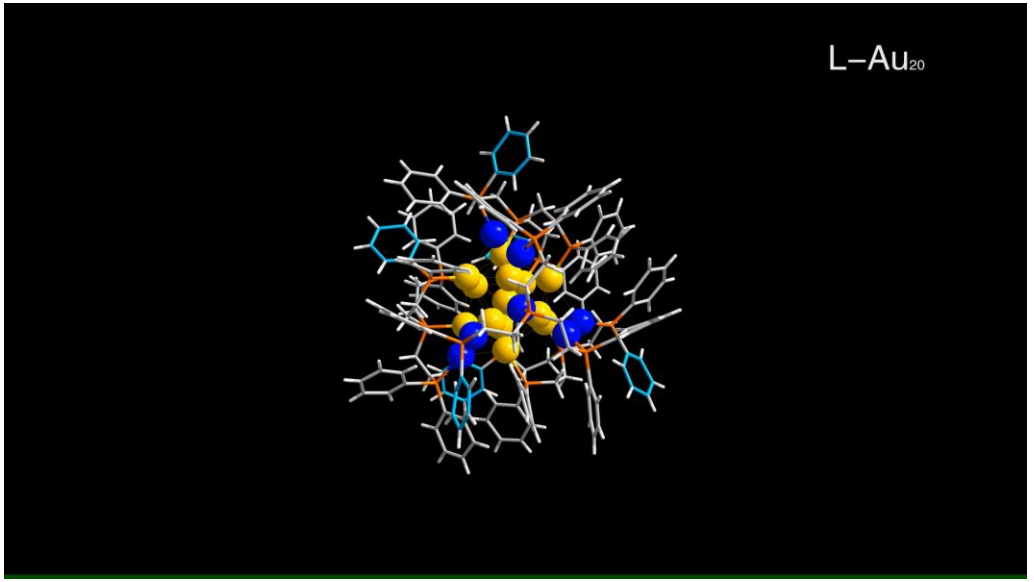

Movie S2. (mp4 format) Movie of molecular docking and quantum-chemistry simulations of the L-Au_{20}(α-CD)$_6$ assembly process.

Conclusions

- In summary, inspired by the process of chaperonin mediated protein folding with multiple chiral sites, racemic Au_{20} which has an intrinsically chiral core without achiral environment has been separated via supramolecular assembly with α -CD in a high enantiopurity and large yield.

- The inherent chirality endows the as-separated Au_{20} enantiomers with unique optical activity originating from the electronic transitions inside the cores, which is clearly different from other metal clusters that have large contributions from charge transfer between ligands and metal centers.

- The favorable configurations of R-Au_{20}(α-CD)$_n$ assemblies, in which more O···H attraction bonds form and thus result in stronger binding energy, is found to be responsible for efficient enantioseparation.

- This supramolecular assembly strategy opens the new avenue towards facile separation of chiral nanomaterials via multiple weak interactions, which will greatly benefit the application of chiral materials in the field of optics, catalysis and magnetics.

Thank You

Questions?